Short-term Solar Irradiance Prediction from Sky Images with a Clear Sky Model ——Supplementary Material——

Huiyu Gao and Miaomiao Liu
Australian National University, Canberra, Australia
{huiyu.gao, miaomiao.liu}@anu.edu.au

1. Implementation Details

Tab. 1 summarises the the training setup and parameters in our transformer-based network. Following [3], we leverage auxiliary information, such as air temperature, relative humidity, wind speed, air pressure, azimuth angle, zenith angle and solar irradiance from a clear sky model [2] in our nowcasting network. Different from [3], we include the date d and minute m for each image which benefit the results.

Our transformer-based nowcasting network takes as input an image and the auxiliary data which are of size $(224\times224\times3)$ and (9×1), respectively. We extract the feature representation $\mathbf{f} \in \mathbb{R}^{64}$ for each image from the nowcasting network. The structure of our transformer encoder module follows [1]. For the residual prediction module, we show the feature dimensions from different layers in Fig. 1.

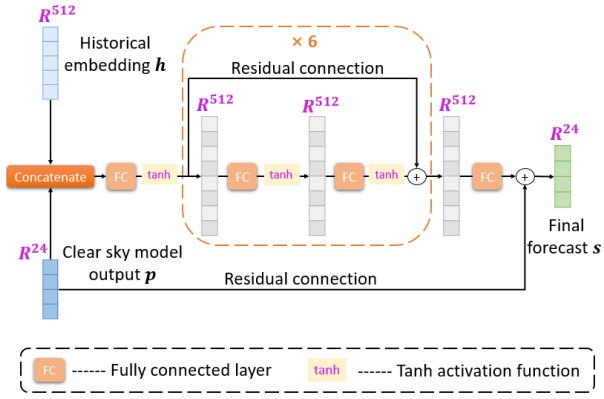

Figure 1. Structure of our residual prediction module.

Both our nowcasting and forecasting networks are trained using the SGD optimizer with a momentum of 0.9. We use a learning rate of 0.001 with a warmup for the first 500 steps and a cosine decay starting at the 501 step. The network is trained for 50000 steps in total.

Parameter	Value
Sky image I	$224 \times 224 \times 3$
Auxiliary data $\mathbf{a}$	9×1
Feature representation f	64×1
Estimated solar irradiance e	1×1
Historical embedding $\mathbf{h}$	512×1
Initial prediction $\mathbf{p}$	24×1
Final forecast $\mathbf{s}$	24×1
Transformer layers L	12
Extra/Patch embedding $\mathbf{x}_n$	768×1
Encoder input dimension D	768
Encoder input number (nowcasting)	197
Encoder input number (forecasting)	7
Number of attention heads h	12
Dimension in attention blocks d_k	64
Transformer dropout rate	0.1
Dimension in residual blocks	512

Table 1. Size of features and parameters in our network.

2. Additional Visualizations

In Fig. 2 and Fig. 3, we show more nowcasting and forecasting results on TSI880 and ASI16 datasets, respectively. Compared with the results of [3], our method better matches the ground truth on the nowcasting task and achieves superior performance on the forecasting task. In Fig. 4, we visualize more attention maps output by our transformer-based nowcasting network on TSI880 and ASI16 datasets, which further demonstrate our transformer-based nowcasting network can find the most relevant pixels when estimating the solar irradiance from sky images.

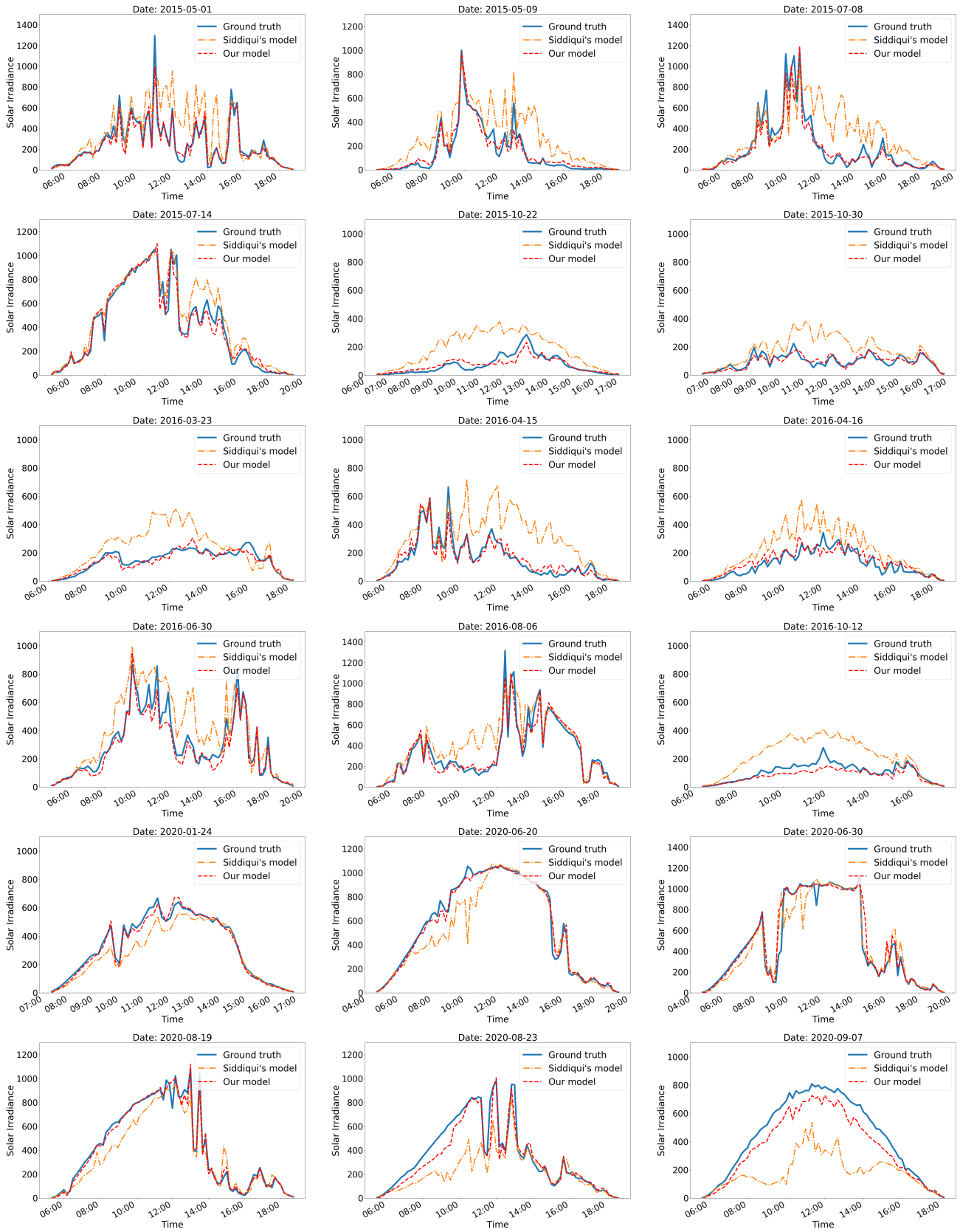

Figure 2. Sampled nowcasting results of solar irradiance on TSI880 2015 dataset (first two rows), TSI880 2016 dataset (middle two rows), ASI16 2020 dataset (last two rows) by Siddiqui's model [3] and our model.

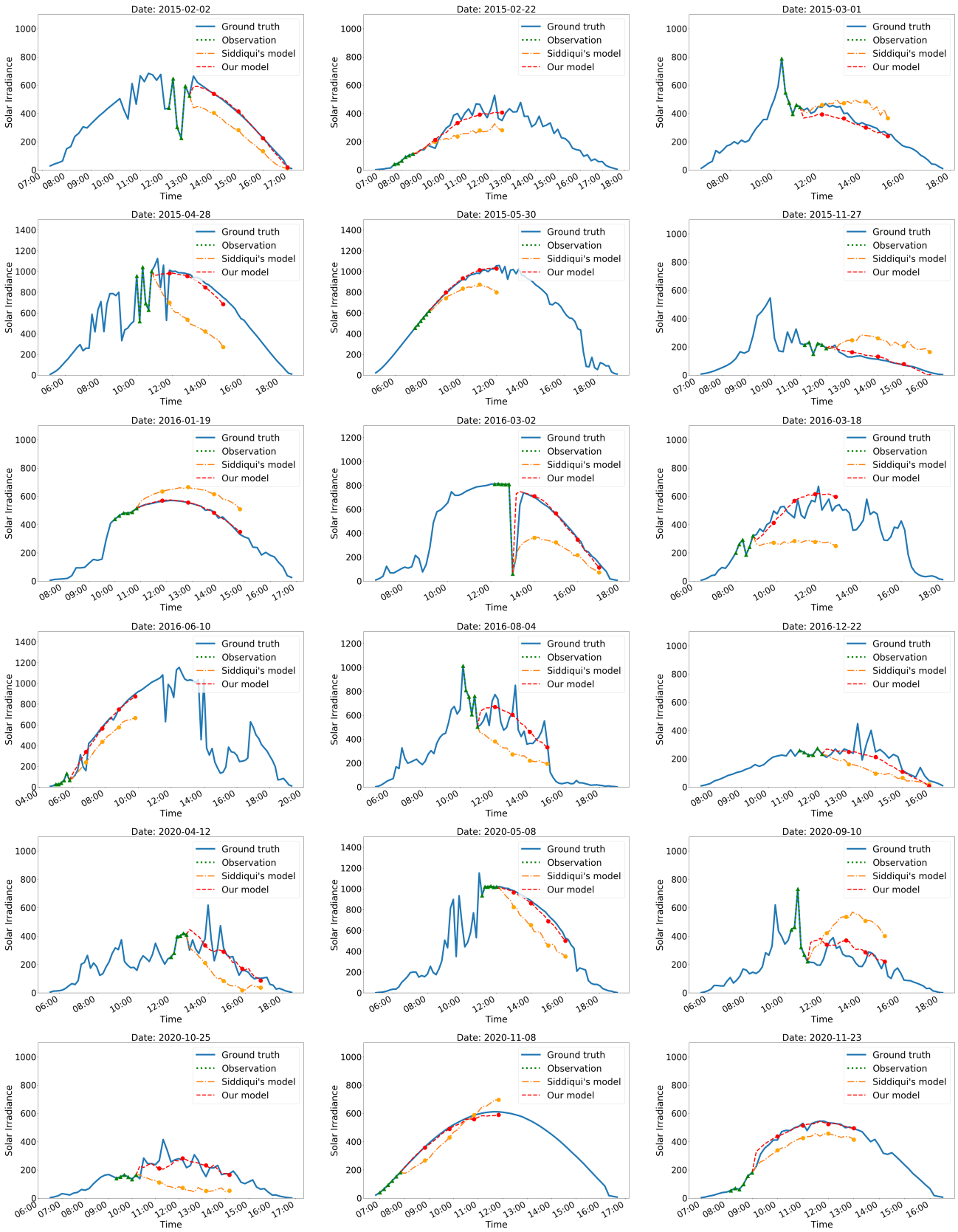

Figure 3. Sampled forecasting results for the next 4 hours on TSI880 2015 dataset (first two rows), TSI880 2016 dataset (middle two rows), ASI16 2020 dataset (last two rows) by Siddiqui's model [3] and our method. The four dots shown on each forecasting curve represent the predicted value exactly at +1h, +2h, +3h, +4h.

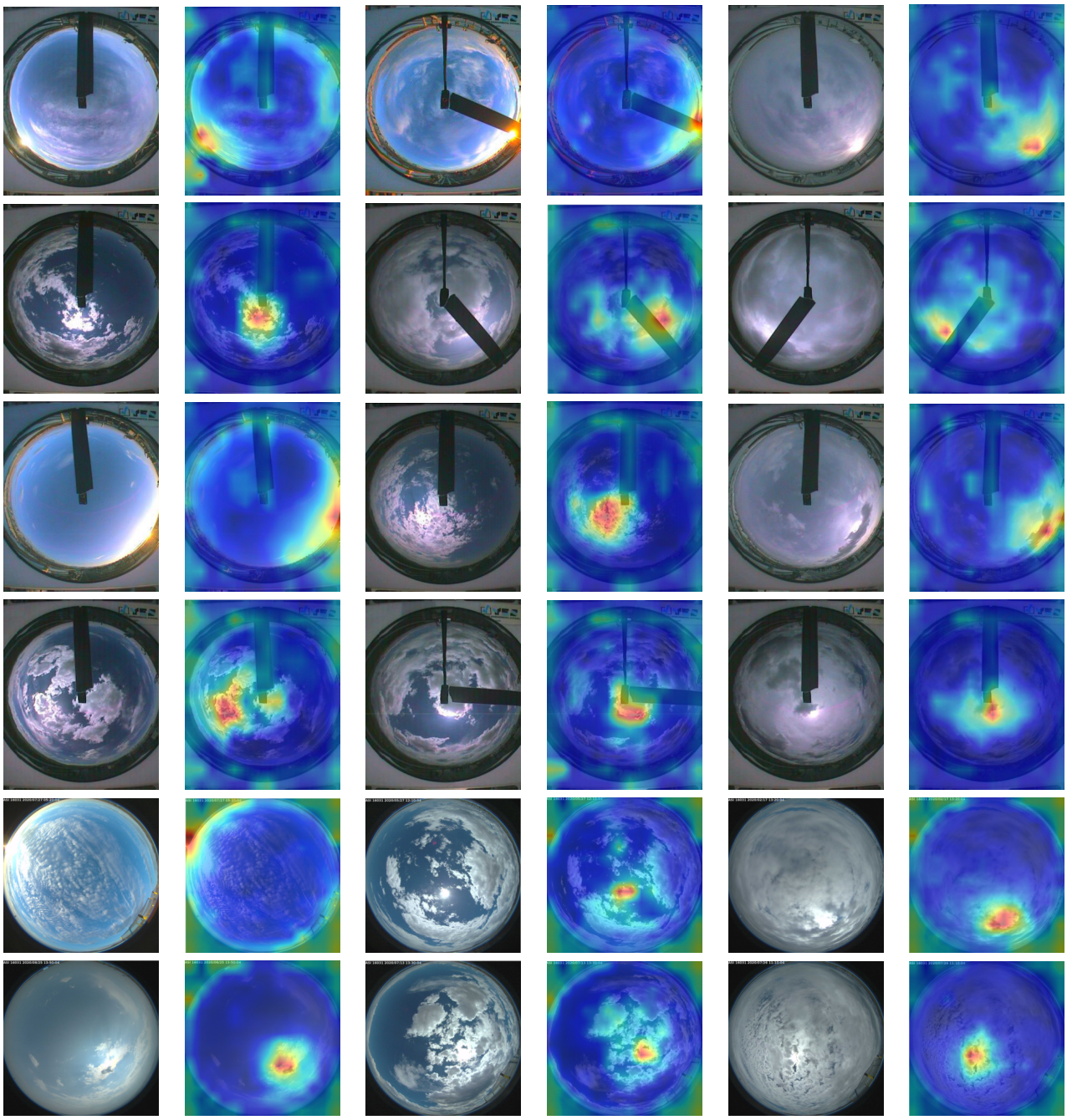

Figure 4. Visualization of sky images as well as their corresponding attention maps by our transformer-based nowcasting network on TSI880 2015 dataset (first two rows), TSI880 2016 dataset (middle two rows), ASI16 2020 dataset (last two rows)

References

[1] Alexey Dosovitskiy, Lucas Beyer, Alexander Kolesnikov, Dirk Weissenborn, Xiaohua Zhai, Thomas Unterthiner, Mostafa Dehghani, Matthias Minderer, Georg Heigold, Sylvain Gelly, et al. An image is worth 16x16 words: Transformers for image recognition at scale. *arXiv preprint arXiv:2010.11929*, 2020.

[2] Bernhard Haurwitz. Insolation in relation to cloudiness and cloud density. *Journal of Atmospheric Sciences*, 2(3):154–166, 1945.

[3] Talha Ahmad Siddiqui, Samarth Bharadwaj, and Shivkumar Kalyanaraman. A deep learning approach to solar-irradiance forecasting in sky-videos. In *2019 IEEE Winter Conference on Applications of Computer Vision (WACV)*, pages 2166–2174. IEEE, 2019.